pH-controlled assembly of DNA tiles

Alessia Amodio, Abimbola Feyisara Adedeji, Matteo Castronovo, Elisa Franco, and Francesco Ricci

Supporting Information

MATERIALS AND METHODS

Reagent-grade chemicals, including tris-base, glacial acid acetic, sodium chloride, magnesium chloride, ethylenediaminetetraacetic acid, ethanol and acetone (all from Sigma-Aldrich, St Louis, Missouri) were used without further purifications. HPLC purified oligonucleotides were purchased from IBA (Gottingen, Germany) and employed without further purification. The following oligos modified and non-modified were used:

Protected tile [1-2] (Fig. SI1):

t1: 5'-ATACCATAGATCCTGATAGC-3'

t2: 5'-AGCAACCTGAAACCAGAATT-3'

t3: 5'-GAATTCTACTCGTGGATCTATGGTAT-3'

t4: 5'-AGAATTGCGTCGTGGTTGCTAGGTCTCGCTATCACCGATGTG-3'

t4 (labeled): cy3: 5'-AGAATTGCGTCGTGGTTGCTAGGTCTCGCTATCACCGATGTG-(cy3)-3'

t5: 5'-AATTCTGGTTTCACCTTAACGATACC-3'

t6: 5'-CGTTAAGGACGACGCAATTCTCACATCGGACGAGTAG-3'

pH-dependent circuit (Fig. 2):

Fuel (F): 5'-AGCAACCTGAAACCACCCTCTTTTCTTTCCC-3'

Catalyst (C): 5'-TTTTCTTTCCCTCACCATG-3'

Deprotector (D): 5'-ATAGATCCTGATAGCGAGACCTAGCAACCTGAAACCA-3'

Substrate (S): 5'-CATGGTGAGGGAAAGAAAAGAGGGTGGTTTCAGGTTGCTAGGTCTC-3'

Clamp-like triplex forming strand (T): 5'-CCCTTTCTTTTCTCCC-GTTTG-CCCTCTTTTCTTTCCC-3'

Duplex Control: 5'-ATCTTAACGTACTGATTA-ATTCC-CCCTCTTTTCTTTCCC-3'

Reporter (Fig. 2a):

R1: 5'-(cy3)-ATAGATCCTGATAGCGAGAC-3'

R2: 5'- TTGCTAGGTCTCGCTATCAGGATCTATR-(cy5)-3'

Labelled clamp-like triplex forming strand (strand forming complex T):

5'-(cy5)-CCCTTTCTTTTCTCCC-GTTTG-CCCTCTTTTCTTTCCC-(cy3)-3'

Buffer conditions. DNA oligonucleotides were suspended to a final concentration of 100 μM and stored in 0.01 M TRIS + 0.01 M $MgCl_2$, pH 7, at -20° C. In all experiments we used solutions of TAE 1x + 15 mM $MgCl_2$ (starting pH = 8.2) with the pH adjusted with the addition of 1 M HCl or 1 M NaOH. All experiments were performed at 25° C.

Protected tile annealing. The protected tile was prepared as reported elsewhere[2] with nominally correct stoichiometry at 5 μM and annealed with a Bio-Rad Mastercycler Gradient thermocycler. The solution was brought down from 95° C to 20° C at a constant rate over a course of 6 h.

Substrates preparation. All the complexes (Reporter, pH-dependent substrate and pH-independent substrate) used in the experiments were prepared mixing the oligos necessary for the formation of the complex at equimolar concentration in TAE buffer 1x + 15 mM $MgCl_2$ pH 7 and were let to react overnight at room temperature.

Fluorescence measurements. All fluorescence measurements were obtained using a Cary Eclipse Fluorimeter (Varian) with excitation at 548 nM (± 5 nm) and emission at 563 nM (± 5 nm). Strand displacement experiments were performed using a concentration of Reporter (R) of 30 nM, F of 20 nM and 10 nM of initial complex (pH-dependent substrare or pH-independent substrate). The Catalyst strand (C) was added at the selected concentration (from 1 nM to 100 nM) after 10 minutes to allow a stable baseline. The signal increase of Cy3 was followed for 1h after C addition.

pH-dependent self-assembly of DNA tiles. This experiment was performed by adding (PT) 200 nM to a mixture reaction of (pH-dependent substrate or pH-independent substrate, the latter for Control experiment) (220 nM), F (440 nM), Catalyst was added at a concentration of 20 nM in TAE buffer 1x + 15 mM $MgCl_2$ at room temperature. Reaction time, 24 h.

Atomic Force Microscopy. AFM topographic height images of the pH-dependent self-assembly nanotubes with 0 - 4 days reaction time, were acquired using AC mode of MFP-3D Stand-Alone AFM (Oxford Instruments - Asylum research, Santa Barbara, CA, USA). Firstly, 20 μl of 50 μM of pH–dependent self-assembly nanostructures (with respect to reaction time) was deposited onto freshly cleaved mica substrate, fixed over a 150 μl-volume, custom-made liquid cell. The adsorption step lasted for 20 minutes for all pHs. Afterwards, 100 μl of DNA-free TAE/Mg buffer (TAE 1x with 15 mM Magnesium acetate tetrahydrate , with respect to the original pH of the sample) was introduced onto the sample to have enough solution that covers the home-made liquid cell. The imaging parameters were as follow; AFM mode: AC mode in liquid, cantilever type: BL-AC40TS-C2 (a bioLever Mini Silicon tip on nitride lever), resonant frequency: 110 kHZ (as specified by the manufacturer (Olympus, Japan)), spring constant: 0.09 N/m (as specified by the manufacturer), scan rate:1 Hz. We acquired 4 to 6 images, from different location of each substrate, at least 50 μm apart with respect to each other. The topographic images were processed with 2nd order flattening, and analysed using Igor Pro 6.37 A.

Fluorescence microscopy. For fluorescence microscopy imaging the central strand of the tile (t4, see sequence above) was labelled at the 3' end with a cy3 fluorophore. An Axio Scope A1 ZEISS microscope was used. The emitted photons were collected by a 63x, air objective (ZEISS) and a monochrome CCD camera (Axiocam 503 mono - ZEISS). The images were analyzed using ZEN 2 lite (ZEISS) software. A 2 μL drop of 50 nM of the sample was deposited between a clean microscope slide and a coverslip.

Measurement of tile-assembly yield. In order to measure the yield of the tile assembly we applied the following procedure using the data obtained from fluorescence images (see Fig. 3, SI8). By assuming an

average thickness of the glass slide sample of 1.5 μm and calculating the total area of imaging (3672 μm^2) we have calculated the volume of the imaged sample (7.3 pL). We have also assumed that the assembled tiles would equally deposit on the two sides of the glass slide. We have thus calculated the number of tiles from the length of the tubes (see statistical analysis in Fig. SI8) (each tile is 14.3 nm) and assuming that each tube has a fixed diameter of 7 tiles. In order to achieve the total yield of tile assembly we have compared the concentration of assembled tiles obtained with the above-described procedure to the concentration of total tiles in solution (200 nM). Of note, the concentration of total tiles in solution is assumed as equal to the concentration of the strands forming the tile (yield of tile formation from separated strands assumed as 100%).

References

(1) Rothemund, P. W. K., Papadakis, N.; Winfree, E. *PLoS Biol. 2*, **2004**, e424.

(2) Zhang, D. Y.; Hariadi, R. F.; Choi, H. M. T.; Winfree, E. *Nat Comm* **2013**, 4, 1965.

SUPPORTING FIGURES

Figure SI1. Reactive and protected tile. (*left*) RT is made of five synthetic DNA strands that hybridize into a rigid rectangular core characterized by two double helices with a single-stranded five-base overhang (sticky end) at each corner (A, A*, B, B*). The presence of these sticky ends allow the self-assembly of RT. (*right*) In the PT, two of the four sticky ends (A* and B*) are protected with two complementary strands, thus leading to stable, monomeric tiles that cannot self-assemble[1-2].

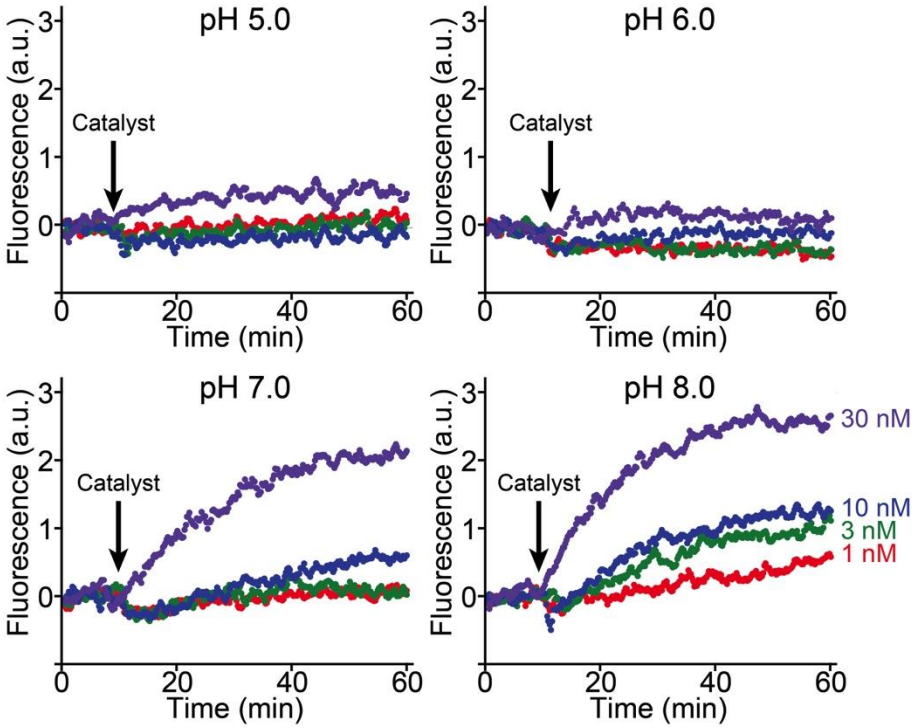

Figure SI2. Upstream pH-dependent strand displacement circuit characterization. The addition of the Catalyst strand (from 1 nM to 30 nM) leads to no significant fluorescence signal change at pH 5.0 and 6.0, thus demonstrating that the formation of sequence specific Hoogsteen interaction at acidic pHs (Figure 2) strongly stabilize the pH-dependent substrate and inhibits the Catalyst-induced strand displacement reaction. In contrast, at neutral/basic pHs (pH 7.0 and 8.0) the destabilization of the Hoogsteen interactions allows successful strand displacement reaction upon the addition of the Catalyst. The kinetic profiles suggest a faster kinetic at pH 8.0. Strand displacement is followed by measuring the fluorescence of a solution of complex pH-dependent substrate (10 nM) and Fuel (F) (20 nM) in the presence of a reporter (R) (30 nM), and after the addition of the Catalyst strand (S) at different concentrations in a TAE 1x buffer + 15 mM $MgCl_2$, at 25° C.

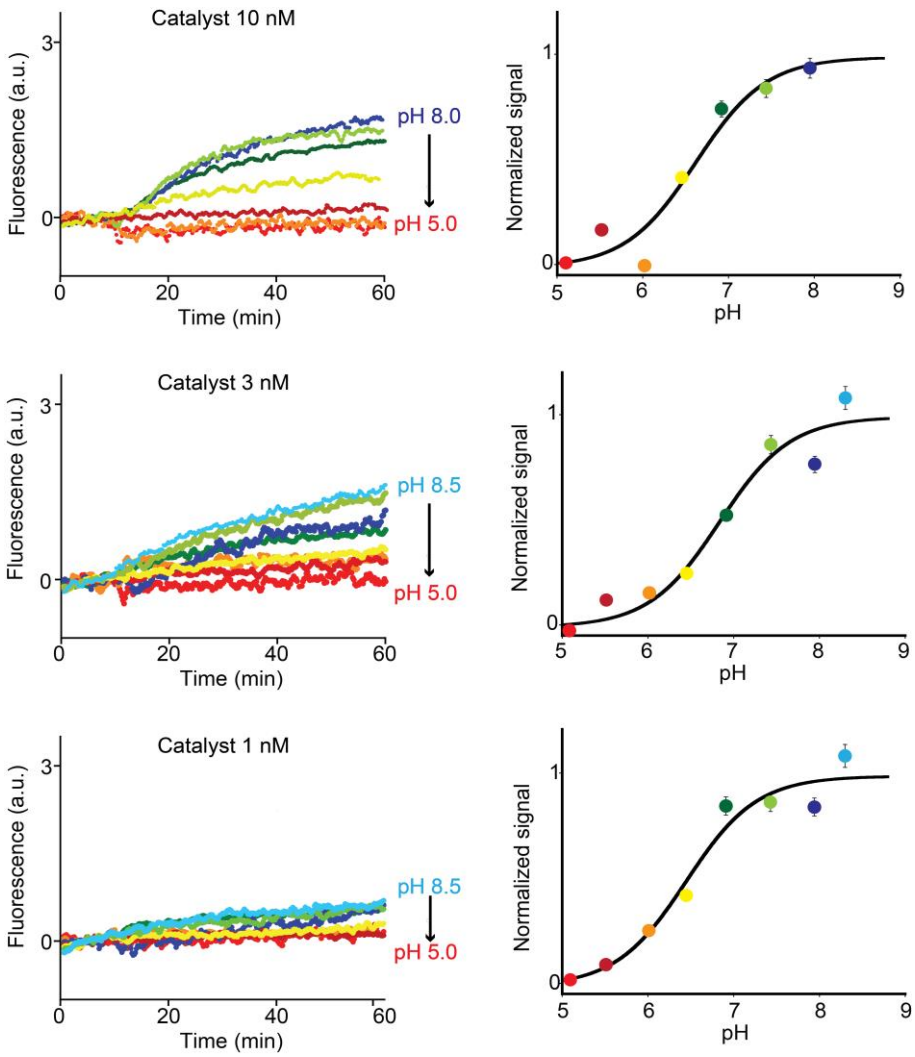

Figure SI3. Upstream pH-dependent strand displacement circuit characterization. We can modulate the upstream strand displacement circuit using both pH and Catalyst concentration. At basic pHs the activation of the strand displacement process can be finely modulated using different concentrations of Catalyst (here are shown three different concentrations: 1, 3 and 10 nM). Strand displacement is followed by measuring the fluorescence of a solution of complex pH-dependent substrate (10 nM) and Fuel (F) (20 nM) in the presence of a reporter (R) (30 nM) (see also Figure 2a), and after the addition of the Catalyst strand (C) at different concentrations in a TAE 1x buffer + 15 mM $MgCl_2$, at 25° C. The normalized signal shown in graph on the right are obtained by using the fluorescence value obtained at t = 60 min in the kinetic experiments shown in the left. Standard deviation is within 5% for all data.

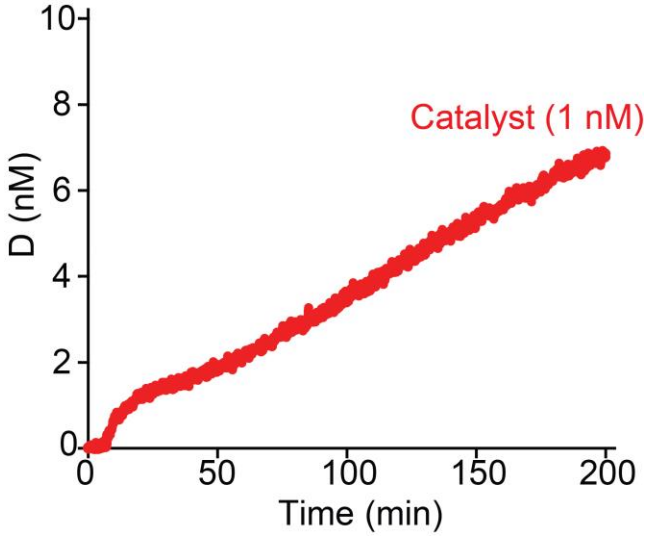

Figure SI4. Characterization of the catalytic efficiency of the upstream circuit upon the addition of the Catalyst (C). The addition of the Catalyst (1 nM) to a mixture containing complex pH-dependent substrate (10 nM) and Fuel (F) (20 nM) in the presence of a reporter (R) (30 nM) strand and under optimal pH conditions (pH 8.0) generates a catalytic response. The turnover number (moles of deprotector formed / moles of catalyst) of this catalytic circuit can be estimated by comparing the signal increase upon Catalyst addition (1 nM) with the signal expected from the addition of the deprotector (y-axis). The turnover number is 4 after 2 hours and 6 after 3 hours from Catalyst addition. This result demonstrates the catalytic efficiency of the upstream circuit to catalytically produce the deprotector strand upon the addition of the Catalyst. We note that the catalytic efficiency appears lower than that observed in the original paper by Zhang et al. (2) probably due to the effect of the triplex-forming tail on the strand-displacement reaction. The experiments were performed in a TAE 1x buffer + 15 mM $MgCl_2$ pH 8.0, at 25° C.

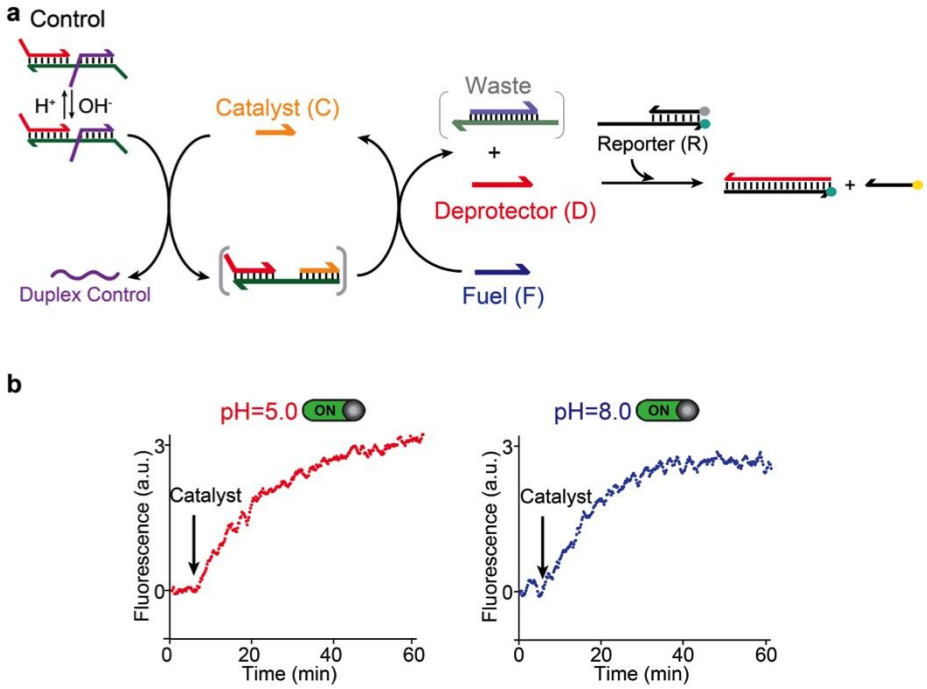

Figure SI5. **pH-independent strand displacement circuit (Control). a)** As a control system we have designed a pH-independent substrate in which the triplex-forming portion of the pH-dependent substrate is substituted with a random tail that is unable to form a triplex structure. We have used an external reporter (R) that stoichiometrically reacts with the released Deprotector strand (D) to give a measurable signal. **b)** We observe an indistinguishable behaviour at both pH 5.0 and pH 8.0 after the addition of the Catalyst strand. Strand displacement is followed by measuring the fluorescence of a solution of complex pH-independent substrate (10 nM) and Fuel (F) (20 nM) in the presence of a reporter (R) (30 nM), and after the addition of the Catalyst strand (S) at a concentration of 30 nM in a TAE 1x buffer + 15 mM $MgCl_2$, at 25° C.

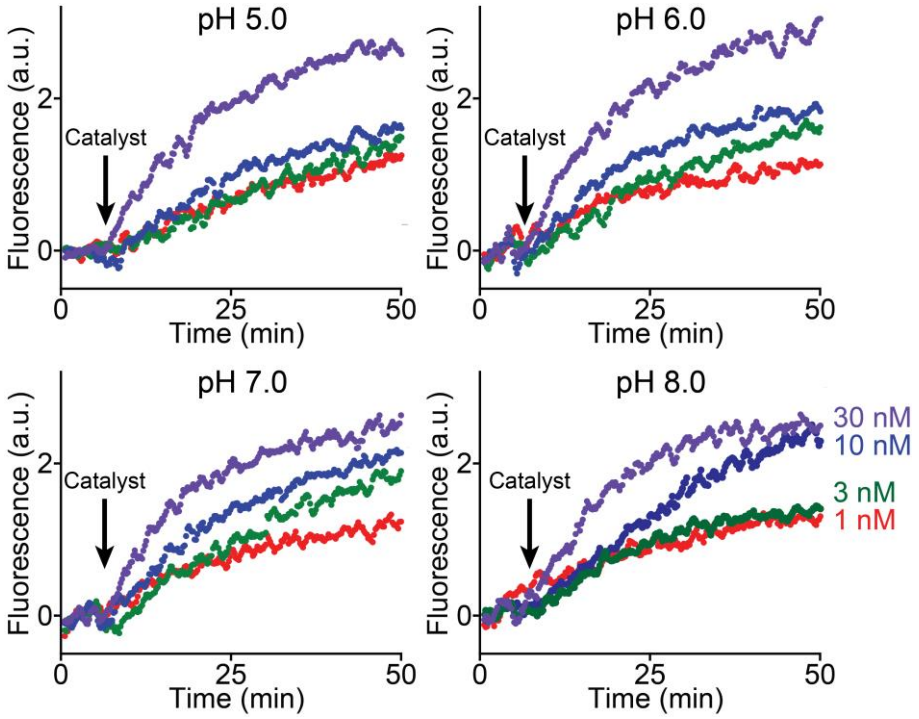

Figure SI6. pH-independent strand displacement circuit (Control). The control pH-independent strand displacement circuit (see Figure SI2) leads to successful release of the Deprotector strand at all the pHs investigated (pH 5.0, 6.0, 7.0, 8.0) with similar kinetic profiles. Strand displacement is followed by measuring the fluorescence of a solution of complex pH-independent substrate (10 nM) and Fuel (F) (20 nM) in the presence of a reporter (R) (30 nM) (see also Figure SI5), and after the addition of different concentrations of Catalyst strand (S) in a TAE 1x buffer + 15 mM $MgCl_2$, at 25° C.

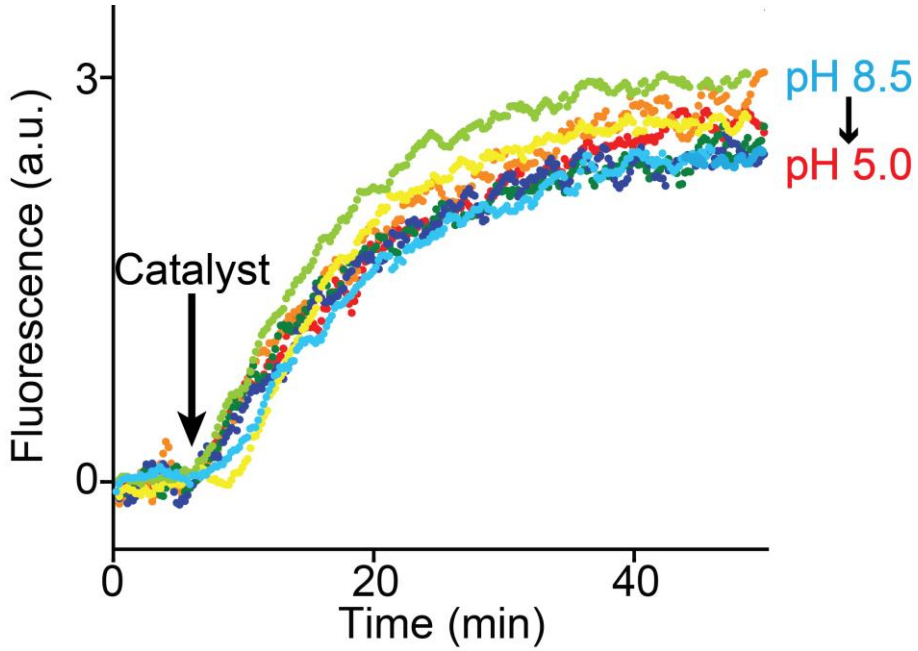

Figure SI7. pH-independent strand displacement circuit (Control). The control pH-independent strand displacement circuit (see Figure SI5) leads to successful release of the Deprotector strand at all the pHs investigated (from pH 8.5 (light blue) to pH 5.0 (red)) with similar kinetic profiles. Strand displacement is followed by measuring the fluorescence of a solution of complex pH-independent substrate (10 nM) and Fuel (F) (20 nM) in the presence of the reporter (R) (30 nM), and after the addition of the Catalyst strand (C) (30 nM) at different pHs in a TAE 1x buffer + 15 mM $MgCl_2$, at 25° C.

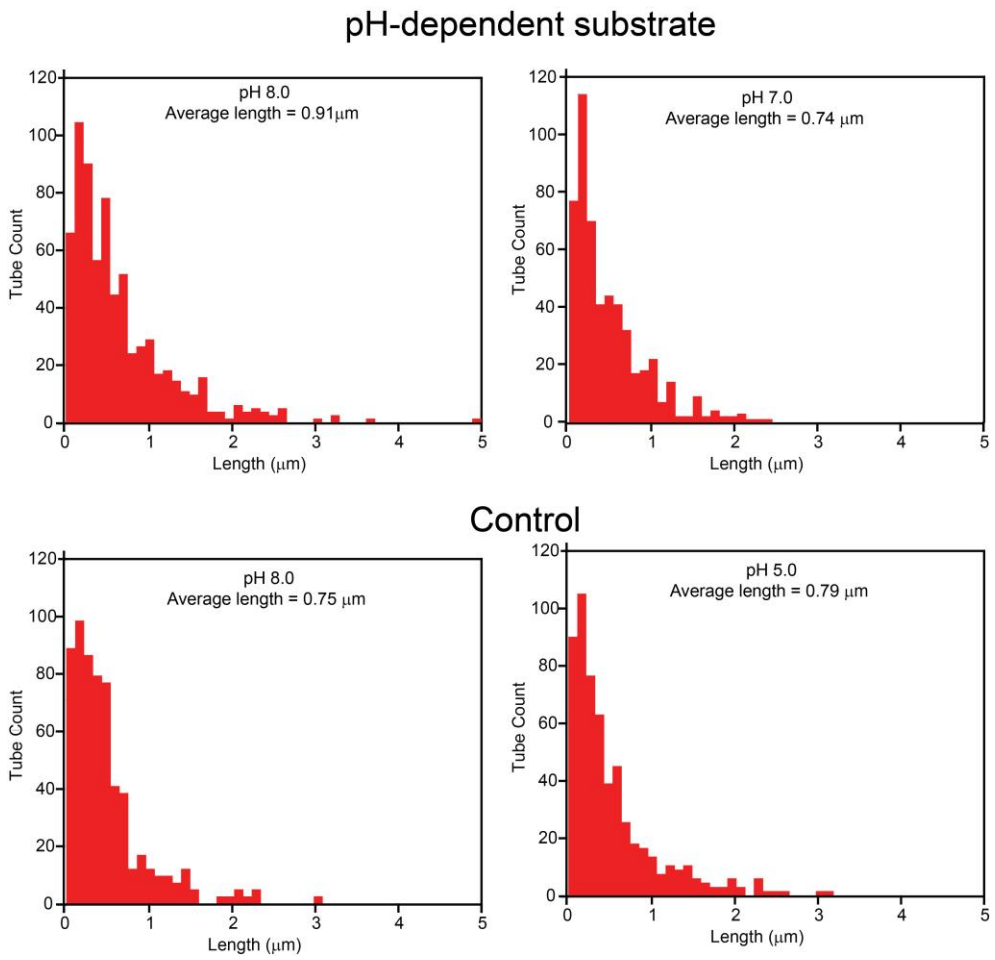

Figure SI8. Statistical analysis of assembled tiles length. The average length of the assembled tiles has been evaluated using fluorescence microscopy images (12 images in total, 3 for each type of reaction). This experiment was performed by adding (PT) 200 nM to a mixture reaction of (pH-dependent substrate or pH-independent substrate, the latter for Control experiment) (220 nM), F (440 nM), Catalyst was added at a concentration of 20 nM in TAE buffer 1x + 15 mM $MgCl_2$ at room temperature. Reaction time = 24 h. The total number of assembled tiles analyzed is: pH-dependent substrate pH 8 = 579; pH-dependent substrate pH 7 = 526; Control pH 5 = 379 and Control pH 8 = 255.

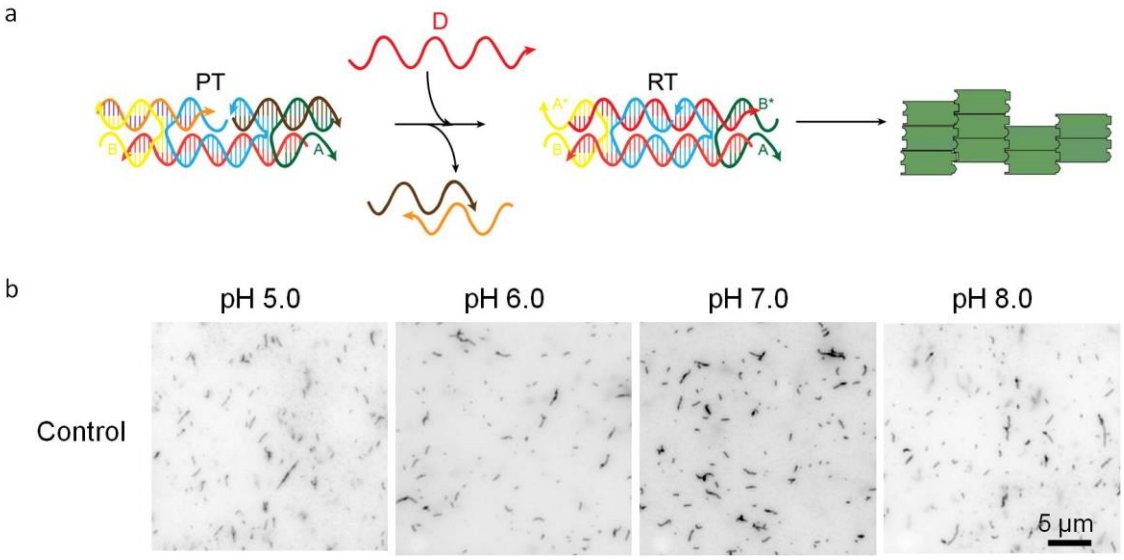

Figure SI9. Control of pH-dependence of DNA tile self-assembly reaction. To demonstrate that DNA tile self-assemble with similar efficiency over the entire pH range tested, we have performed a control experiment in which the Deprotector strand (D) has been exogenously added to a solution of Protected Tiles (PT). **a)** The Deprotector (D) reacts with the Protected Tiles (PT) by displacing the two protectors strands and thus exposing the other two sticky ends. In turn, strand displacement leads to the formation of readily Reactive Tiles (RT) that isothermally form DNA nanotubes. **b)** Fluorescence microscopy of the above control experiment shows that self-assembly of DNA tiles occurs at all the pHs investigated (pH 5.0, 6.0, 7.0, 8.0). Experiments were performed by using a concentration of the Protected Tile of 200 nM and a concentration of the Deprotector strand of 220 nM in TAE 1x buffer + 15 mM $MgCl_2$, at 25° C.

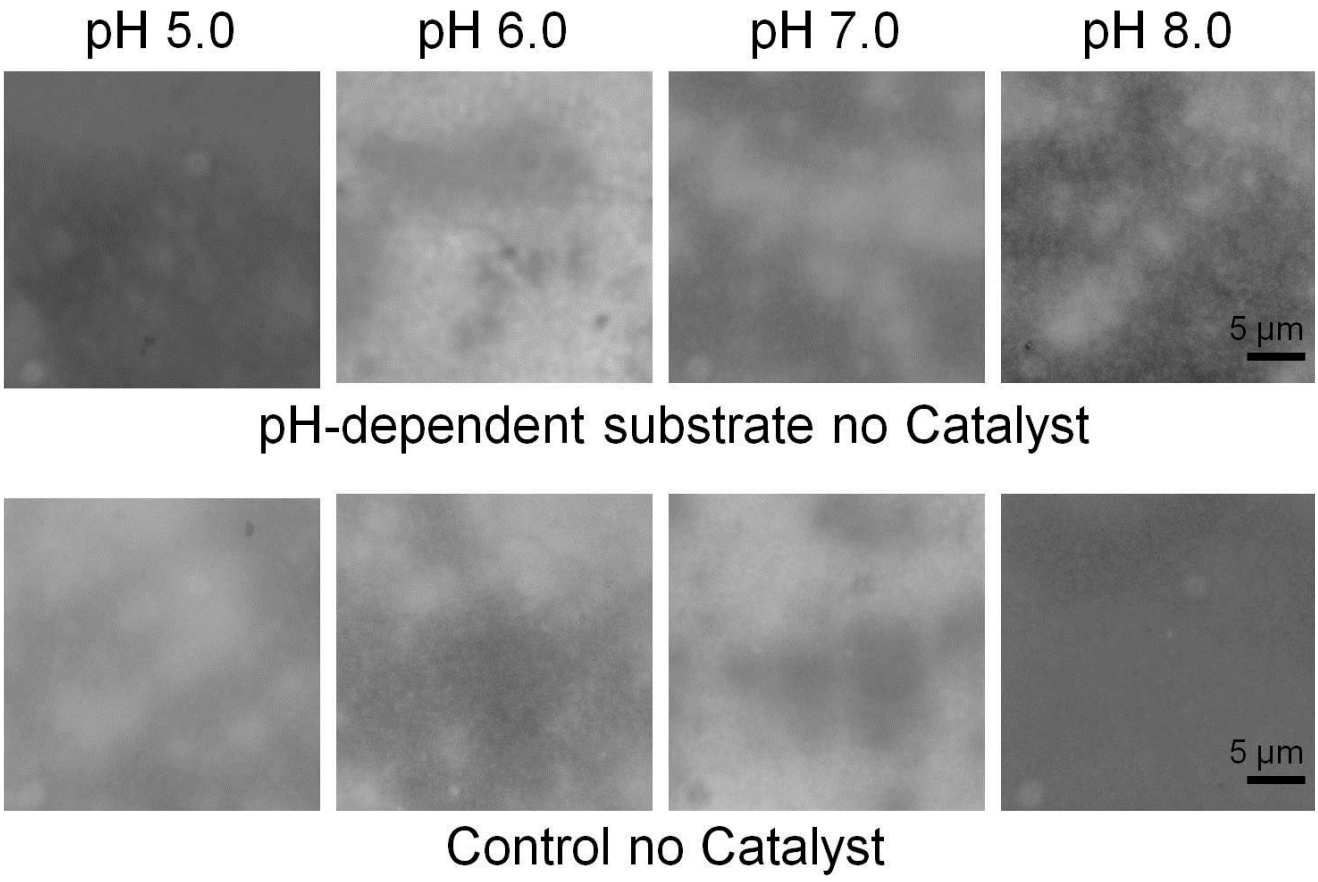

Figure SI10. Fluorescence microscopy images of the integrated reaction network in the absence of Catalyst. In the absence of the Catalyst strand no self-assembly of DNA tiles is observed for all the pHs investigated (pH 5.0, 6.0, 7.0, 8.0) using both the pH-dependent circuit and the pH-independent control circuit. All the experiments were performed with the same concentration of reagents: PT (200 nM), F (440 nM), pH-dependent substrate / pH-independent substrate (220 nM), in TAE 1x buffer + 15 mM $MgCl_2$, at 25° C. For all the fluorescence microscope experiments, a cy3-modified version of the tile central strand (t4, see Material) was used.

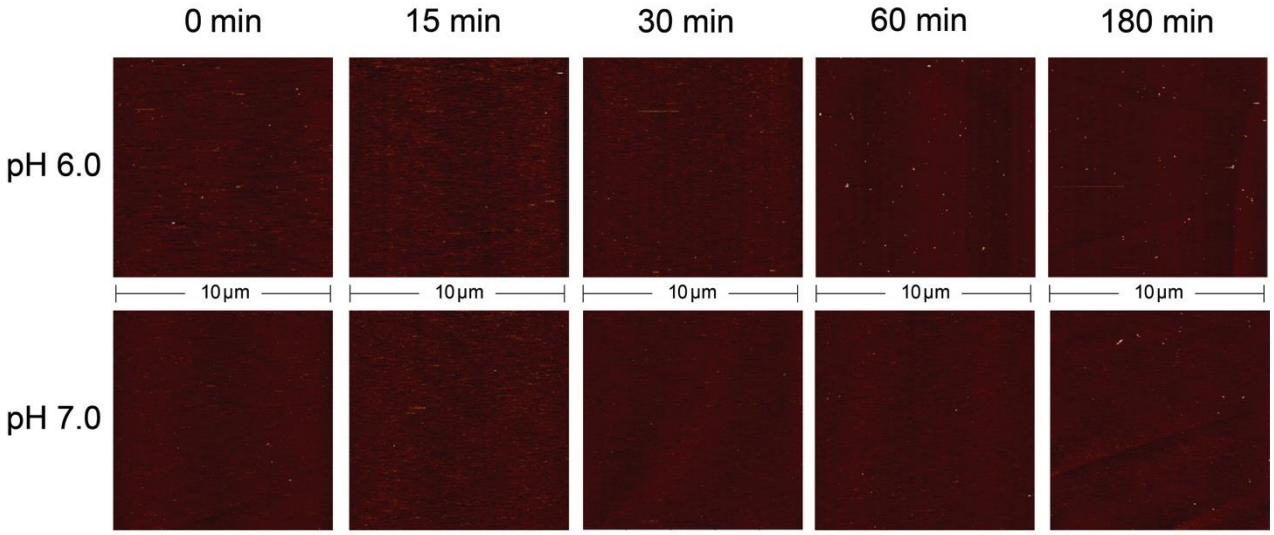

Figure SI11. Kinetic of the pH-dependent nanotubes self-assembly. Kinetic of the integrated system at pH 6.0 (*first row*) and pH 7.0 (*second row*). All the experiments were performed with the same concentration of reagents: PT (200 nM), F (440 nM), pH-dependent substrate (220 nM) and C (20 nM), in TAE 1x buffer + 15 mM $MgCl_2$, at 25° C.

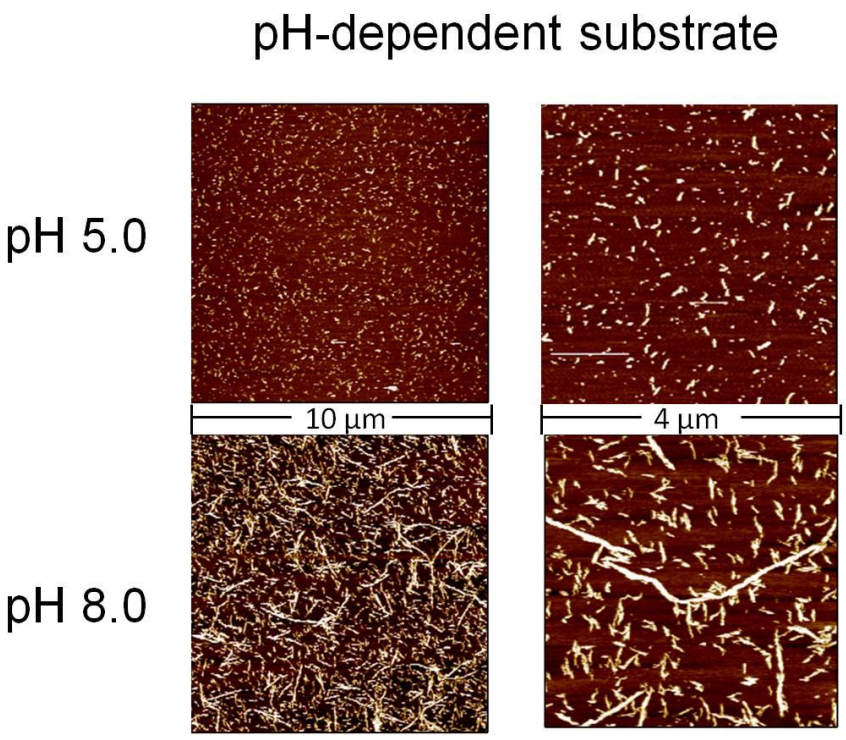

Figure SI12. AFM characterization after 4 days of incubation. The self-assembly of DNA tiles was evaluated by AFM images after 4 days of incubation. We note that assembly of small lattices at pH 5.0 (top raw) is observed under AFM after 4 days since the start of the reaction, presumably due to leak of the Deprotector from the substrate[1]. At the same reaction time we observe DNA nanotubes formation at pH 8 (bottom row). Experiments were performed with the following concentrations of reagents: PT (200 nM), F (440 nM), pH-dependent substrate (220 nM) and C (20 nM), in TAE 1x buffer + 15 mM $MgCl_2$, at 25° C.